Small-angle neutron scattering (SANS) characterization of 13.5 Cr oxide dispersion strengthened ferritic steel for fusion applications

R. Coppola[a,*], M. Klimenkov[b], R. Lindau[b], G. Mangiapia[c]

[a] ENEA-Casaccia, FSN-ING, Via Anguillarese 301, 00123 Roma, Italy
[b] KIT-IAM, Hermann-von-Helmholtz-Platz 1, 76344 Eggenstein-Leopoldshafen, Germany
[c] Heinz Maier-Leibnitz (FRM II) - Helmholtz Zentrum Geesthacht, Lichtenbergstr. 1, D-85748 Garching b., München, Germany

ARTICLE INFO

ABSTRACT

Small-angle neutron scattering (SANS) has been utilized for micro-structural investigation on laboratory heats of oxide dispersion strengthened (ODS) 13.5 Cr wt % ferritic steel, with 0.3 wt% Y_2O_3 and with variable Ti and W contents. The results show that increasing the Ti content from 0.2 to 0.4 wt% a distribution of nano-clusters develops, tentatively identified as $Y_2Ti_2O_7$, with average radii as small as 6.5 Å and volume fractions increasing from 0.021 to 0.032. The measured SANS cross-sections show also the growth of much larger defects, possibly Cr oxides. Furthermore, the ratio of magnetic to nuclear SANS components shows that the defect composition varies both with their size and with the Ti and the W content. These results are in qualitative agreement with transmission electron microscopy (TEM) observations, showing a striking influence of Ti addition on particle size refinement. However, while TEM is limited in statistics and minimum observable size of the Ti-rich nano-clusters, the defect distributions obtained by these SANS measurements provide complementary information useful for morphological characterization of the micro-structure in the investigated material.

1. Introduction

Compared to traditional ferritic/martensitic steels, oxide dispersion strengthened (ODS) steels, containing high volume fractions of uniformly distributed oxide nano-clusters, offer higher performance under severe service conditions, namely better resistance to irradiation degradation and to thermal creep deformation at operating temperatures up to 800 °C [1,2]. In fact, the diversified distribution of nano-clusters and other nano-scale micro-structural features results in a high point defects sink strength, providing strong reduction in void swelling and embrittlement, compared to ferritic/martensitic steels [2]. ODS ferritic/martensitic steels are therefore attractive candidates as structural materials both for DEMO relevant applications [3] and for Gen IV reactor technology [4]. However, methodologies for fabrication of industrial heats are not yet fully developed, experimental work is needed to optimize production routes, check mechanical properties, understand micro-structural evolution. Concerning more specifically micro-structure, the metallurgical efforts to produce nano-clusters distributions capable to really improve the performance of such steels require a deep characterization to check reproducibility of the adopted fabrication methods and to understand how the non-magnetic precipitates or nano-clusters develop inside the ferritic/martensitic matrix. This is essential

not only to validate the adopted production route in the as-received material, but even more in view of its utilization under irradiation.

Within this frame, a purely ferritic ODS steel has been developed modifying the Eurofer97 steel composition in such a way as to avoid phase transformation in the fusion relevant operational plant temperature range [5–9]. Namely, with respect to Eurofer97 the Cr content has been increased and fixed Y_2O_3 has been added, together with different Ti and W contents, in the aim of optimizing the distribution of nano-clusters; the correlation of mechanical properties of these laboratory heats with their micro-structures was then investigated by transmission electron microscopy (TEM), X-ray diffraction, energy-dispersive X-ray spectroscopy (EDX), electron energy loss spectroscopy (EELS) and atom probe tomography atomic probe. The here above quoted papers, and more specifically Ref. [6] showed the role of the Ti content in refining the nano-clusters distributions, but with severe statistical limitation for the ultrafine nano-clusters, smaller than 20 Å and with difficulties in identifying the exact composition of the Y-Ti-O complexes. Therefore, small-angle neutron scattering (SANS) measurements were carried out on samples obtained from the same laboratory heats investigated by the techniques mentioned here above. In fact, SANS probes volumes of approximately 0.1 cm^3, that is several orders of magnitude larger than those investigated by X-ray diffraction

or electron microscopy; consequently, the micro-structural information obtainable by this technique is averaged over volumes comparable to those involved in mechanical testing. On the other hand, SANS is an indirect technique, requiring reliable metallurgical information from other experimental methods, or from theory, for a correct exploitation when applied to complex materials, such as these ODS ferritic/martensitic steels. Therefore, the interpretation of the SANS results presented in this paper is not intended as a conclusive one, but as a contribution, based on the current knowledge of these materials, to better characterize their micro-structure and to progress in obtaining quantitative information about its development.

2. Material characterization

The investigated laboratory heats had been prepared modifying the composition of Eurofer97 (0.12C, 9 Cr, 0.48 Mn, 0.2 V, 1.08 W, 0.14 Ta wt%) with the addition of 0.3 wt% Y_2O_3, increasing the W content to 2.0 wt% and adding three different contents of Ti, namely 0.2 wt%, 0.3 wt% and 0.4 wt%. A Ti free heat was also prepared to serve as reference in investigating the effect of increasing Ti content. Additionally, a laboratory heat with 1.1 W and 0.3 Ti wt % was prepared, since an optimum effect on particle size refinement had been observed for this Ti content [6,7]. Table 1 lists the compositions of the investigated samples. These heats were produced by mechanical alloying and subsequent heat treatment (2 h at 1050 °C), obtaining practically fully compacted materials with a negligible porosity [6]. Furthermore, these TEM observations showed a complex micro-structure. In fact, an originally uniform distribution of grains several μm large, when adding Ti is modified into a bi-modal one, with grains smaller than 5000 Å. Always quoting the results published in Ref. [6], spherical precipitates, with size ranging between 500 Å and 3000 Å were observed both before and after adding Ti and identified as Cr oxides by means of EELS and EDX. Much smaller spherical particles were detected in the Ti free material, consisting mainly in Y and O, possibly yttria clusters. Adding Ti, produced even finer clusters, smaller than 300 Å in size, interpreted by means of EELS and EDX as Y-Ti-O complexes like $Y_2Ti_2O_7$ [6]. However, the TEM characterization of such small defects in a magnetic matrix is challenging particularly for sizes smaller than 20 Å, since they are nearly invisible by this technique; consequently, it is also difficult to make clear conclusions on the exact chemical composition of these defects, namely to confirm that the Y, Ti and O contents are the same for all of them, or exclude that other elements such as Cr or Fe are included in their composition. Additional atom probe characterization of these same laboratory heats [9] confirmed that Ti addition enriched the chemical composition of clusters as large as at least 30 Å.

3. Experimental technique and data analyis

General information on application of the SANS technique in materials science can be found in Refs. [10,11] and in Ref. [12] concerning more specifically ODS alloys for nuclear applications. Previous SANS results of Eurofer97 ODS steel are reported in Refs. [13,14]. The samples for SANS investigation were prepared as polished platelets approximately 1 cm² in surface area and 1 mm thick, obtained from the same material utilized for the other micro-structural investigations. An

Eurofer97 sample measured in a previous SANS experiment [13] was also measured for comparison; it had been subjected to standard treatment at 1040 °C for 30′ + 760 °C for 1.5 h. The SANS measurements were carried out at the D22 diffractometer at the High Flux Reactor of the Institut Laue–Langevin (ILL) in Grenoble, France [15]. A neutron wavelength λ = 6 Å and sample-to-detector distances of 2 m and 11.2 m were selected in order to cover a range of the scattering vector $Q = 4\pi \sin\theta/\lambda$ (2θ full scattering angle) between 3 x10^{-3} to 0.26 Å^{-1}; it corresponds to defect sizes varying between 10 Å and 500 Å approximately. Calibration to absolute values was obtained through the ILL standard data reduction programs [16]. An external, horizontal magnetic field of 1.5 T was applied to the samples in order to saturate their magnetization and measure the nuclear and the magnetic SANS components separately. In fact, for magnetic samples the total SANS cross-section (where Ω stands for the solid angle) is

$$\frac{d\Sigma(Q)}{d\Omega} = \left(\frac{d\Sigma(Q)}{d\Omega}\right)_{nucl} + \left(\frac{d\Sigma(Q)}{d\Omega}\right)_{mag} \sin^2\alpha \tag{1}$$

where α is the azimutal angle on the detector plane. Parallel to the magnetic field (α = 0°) the nuclear SANS cross-section is measured, perpendicular to it (α = 90°) the sum of the nuclear and magnetic ones is measured. Therefore, their ratio R(Q) (also defined "A" in the literature)

$$R(Q) = \frac{(d\Sigma(Q)/d\Omega)_{nucl} + (d\Sigma(Q)/d\Omega)_{mag}}{(d\Sigma(Q)/d\Omega)_{nucl}} = 1 + \frac{(\Delta\rho)^2_{mag}}{(\Delta\rho)^2_{nucl}} \tag{2}$$

is related to the composition of the micro-structural defects, $(\Delta\rho)^2$ being the "contrast" or square difference in neutron scattering length density (nuclear and magnetic respectively) between the observed nuclear and magnetic defects and the matrix. Also due to its quadratic dependence on neutron scattering length densities, identical values of R (Q) may correspond to different defect chemical or magnetic compositions, therefore its interpretation may not be unambiguous without additional information on defect compositions. In general, a value of R (Q) constant over all the explored Q range should imply that the composition of the defects is the same, while its dependence on Q should be associated with the presence of different defect compositions, relating to their sizes.

The distributions of the scattering defects are obtained by inverse transformation of the SANS cross-sections. Namely, if their volume fraction is low and there is no inter-particle interference, the SANS nuclear and magnetic cross-sections can each one be written as

$$\frac{d\Sigma(Q)}{d\Omega} = (\Delta\rho)^2 \int_0^{+\infty} N(R)[V(R)]^2 |F(Q, R)|^2 dR \tag{3}$$

where N(R) is the number per unit volume of defects with a size between R and R + dR, V their volume, $|F(Q, R)|^2$ their form factor (assumed spherical in this case).

The volume distribution function D(R), average defect radius, < R > , and volume fraction, f, are defined respectively as follows:

$$D(R) = N(R)R^3 \tag{4}$$

$$\langle R \rangle = \frac{\int_0^{+\infty} N(R)R dR}{\int_0^{+\infty} N(R)dR} \tag{5}$$

$$f = \frac{\int_0^{+\infty} N(R)V(R)dR}{(\Delta\rho)^2 V_{tot}} \tag{6}$$

where V_{tot} is the total volume of the investigated sample.

A simple transformation method to determine N(R) is presented in Ref. [17]. It has been recently improved for studying radiation effects in Eurofer97 [18,19]. This fitting procedure assumes no *a-priori* shape of

Table 1
Chemical composition of the investigated samples (wt%, Fe bal).

Cr	W	Ti	Y_2O_3
13.5	2.0	0	0.3
13.5	2.0	0.2	0.3
13.5	1.1	0.3	0.3
13.5	2.0	0.3	0.3
13.5	2.0	0.4	0.3

the defect distribution, representing it by a set of cubic B-spline functions, with knots uniformly distributed in a log$R$ scale and with the constraint $N(R) > 0$. The number of splines is chosen taking into account the R-range $R_{min.} - R_{max}$ where the size distribution has to be investigated and the shape of the experimentally determined SANS cross-section. Knots spacing, R-range and a constant or Q-dependent background are additional parameters, adjustable for improving the fit. The best-fit distribution is determined within an 80% confidence band. In general, the main difficulties in obtaining the distributions arise from the fact that the SANS cross-section is measured only on a finite Q-interval, in a limited number of points, affected by experimental errors. Furthermore, a theoretical model distribution usually is not available for complex micro-structural phenomena in such technical steels. All this must be taken into account in selecting the fitting parameters, in order to obtain plausible distributions and, at the same time, reduce their error band as much as possible.

4. Results and discussion

The nuclear SANS cross-sections and $R(Q)$ ratios measured for standard Eurofer97 and for Ti free 2.0 W 13.5 wt% Cr ferritic steel are shown in Fig. 1 a – b respectively. The increase in the SANS cross-section at high Q-values is similar to the one shown in Ref. [13] for ODS Eurofer97: it is attributed to the presence of Y_2O_3 nano-clusters in this Ti-free ODS steel. Its $R(Q)$ ratio (Fig. 1 b) depends markedly on Q: it is possible that for low Q's the measured SANS effect is partly determined by the large Cr oxides. The SANS cross-section and $R(Q)$ measured for Eurofer97 submitted to standard treatment are attributed to carbide precipitates as large as 500 Å, with typical composition $Cr_{14}Fe_8W_{0.7}V_{0.3}C_6$ [18–20].

Fig. 2 a –b shows the nuclear SANS cross-sections and $R(Q)$ ratios of the Ti-free, 2.0 W 13.5 wt% Cr ferritic steel compared to those with Ti contents of 0.2 wt%, 0.3 wt% and 0.4 wt%. The Ti free sample had been prepared as both a TEM and a SANS reference to investigate the effect of increasing Ti contents. However, concerning SANS it is clear from Fig. 2 - a that adding Ti also the distribution of the larger defects, probably Cr oxides, is deeply modified, so that it is not possible to simply subtract the SANS cross-section of the Ti-free sample from the other ones. In fact, adding Ti, the original SANS cross-section of the Ti-free sample is completely modified by a marked increase at high Q values and by significant changes also at the smaller Q values, taking into account that the plot is on logarithmic scale. The so called "Porod behavior" [10,11], that is the asymptotic effect of very large defects following a Q^{-4} trend, is not exactly observed. Furthermore, the $R(Q)$ ratio, and therefore the defect composition, changes with Ti content and defect size (Fig. 2 - b). For the samples with Ti contents 0.2 wt% and 0.4 wt% respectively, over most of the explored Q range it is

relatively constant, with values close to those calculated in Ref. [12] for YTiO, that is 1.9, and for $Y_2Ti_2O_7$, that is 2.54. For the sample containing 0.3 wt% Ti, $R(Q)$ depends markedly on Q and reaches significantly higher values, implying a different composition of the nano-clusters. The effect of this same Ti concentration has been investigated also in a heat containing 1.1% W [6,7]. Fig. 3 a – b show the comparison of the nuclear SANS cross-sections and $R(Q)$ ratios measured for the two different W contents, 2.0 wt% and 1.1 wt%, for same 0.3 Ti wt % content. Decreasing the W content from 2.0 wt% to 1.1 wt%, the nuclear SANS cross-section remains nearly unchanged (Fig. 3 a), but $R(Q)$ (Fig. 3 b) decreases significantly and remains constantly close to the values expected for $Y_2Ti_2O_7$. It appears therefore that for 0.3 wt% Ti content the W content influences significantly the composition of the nano-clusters, but it would be difficult to make more specific statements without examining at least another couple of such samples with identical Ti content and different W contents. It should also be considered that the investigated samples are issued from experimental, laboratory heats, prepared by a non-standardized procedure and therefore possibly subjected to fluctuations in the final elemental composition.

The size and volume distributions have been determined from the nuclear SANS cross-sections shown in Fig. 2 – a; a number of 7 spline functions has been chosen, with $R_{min} = 3$ Å and adding at high Q an adjustable background parameter of a few units in 10^{-3} cm^{-1} to account for the fact that a reference sample is not available. Based on the SANS data analyses published in Ref.s [18,19] this way to proceed for evaluating the background provides anyhow sufficiently reliable results. As shown by the continuous lines in Fig. 2 – a, a good fit has been obtained. The obtained distributions are shown in Fig. 4 a – b; it is noted that since the SANS cross-section is governed by the square volume of the defects (Eq. (3)), the volume distributions provide more significant information on the defects effectively contributing in the measured effect. Based on the TEM results of Ref. [6], it has been assumed that $Y_2Ti_2O_7$ is the dominant composition for the Y-Ti-O nano-clusters. The average radii and volume fractions obtained under this assumption are reported in Table 2. As it is also clear from the SANS cross-sections themselves (Fig. 1 a), with increasing the Ti content there are no significant changes in the average radius. The volume fraction increases with the Ti content, but its evaluation depends on the value of the neutron contrast (Eq. (6)). Therefore a detailed identification of the defects present in each sample, particularly in the one with 0.3 wt% Ti content, would be necessary to more correctly evaluate it. Nevertheless, also considering the SANS cross-sections in Fig. 2 a, it is evident that the distribution of large particles initially present in the Ti free material is completely modified when adding Ti by the appearance of a distribution of much finer particles, most probably Y-Ti-O complexes, well below the resolution limit of TEM [6]. The increase in the volume fraction for the highest Ti content 0.4 wt% reflects the behavior of the
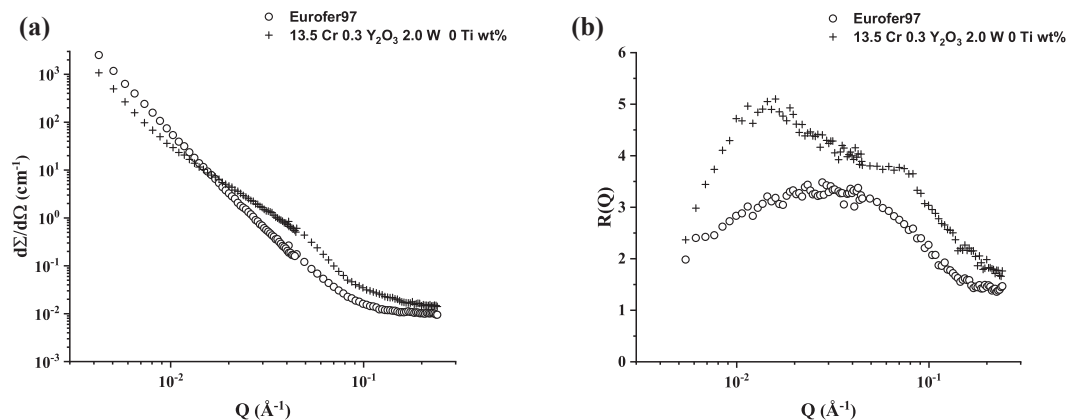

Fig. 1. Nuclear SANS cross-sections (a) and $R(Q)$ values (b) for Eurofer97 submitted to standard treatment (circles) and for ferritic steel Cr 13.5 wt% W 2.0 wt% (crosses).
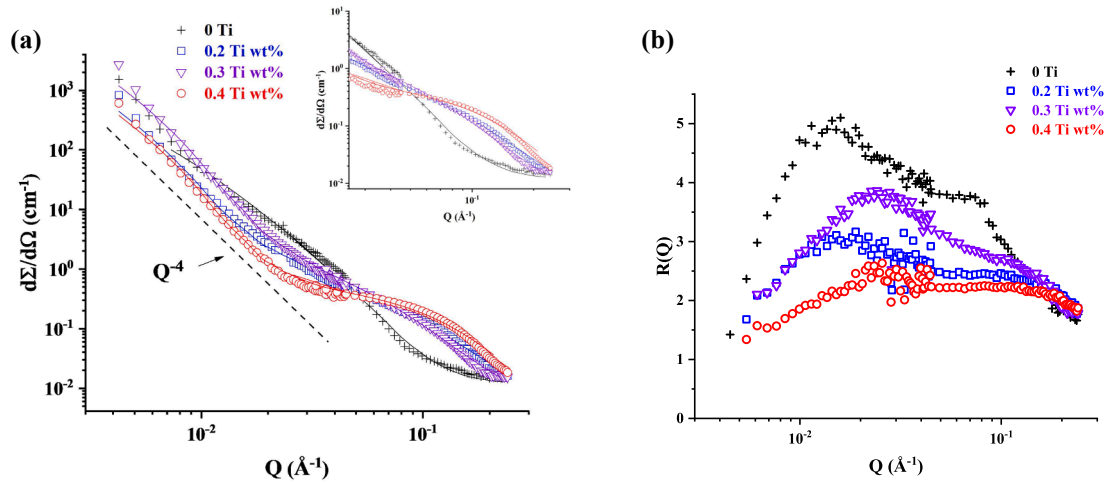
Fig. 2. Nuclear SANS cross-sections (a) and *R(Q)* ratios (b) for 13.5 Cr 2.0 W ODS ferritic/martensitic steel with 0 Ti (crosses, black), 0.2 wt% Ti (squares, blue), 0.3 wt% Ti (triangles, violet), 0.4 wt% Ti (circles, red). The trend corresponding to the "Porod behavior" is indicated by the dotted line. The contnuous lines in (a) represent the best-fits corresponding to the distributions in Fig. 4.
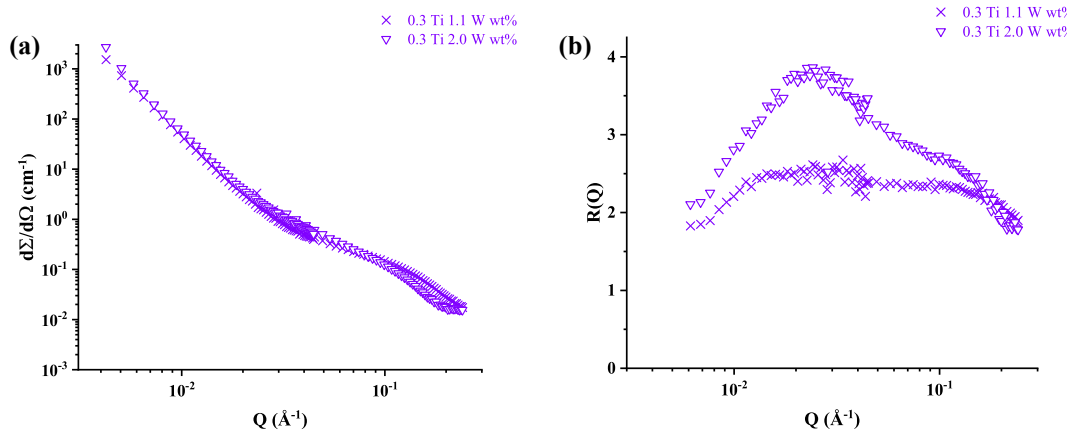

Fig. 3. Nuclear SANS cross-sections (a) and *R(Q)* values (b) for ferritic steel 0.3 Ti wt % Cr 13.5 wt% with W 2.0 wt% (triangles) and with W 1.1 wt% (x).

SANS cross-section measured for $Q > 4 \times 10^{-2}$ Å^{-1} (Fig. 2 a). An enhancement of the small Y-Ti-O complexes development would be the most reasonable explanation, but the exact chemical composition of such defects should be checked, since it might be different for the different Ti contents, changing accordingly the neutron contrast and the value of the volume fraction (Eq. (6)). The secondary defect populations visible in Fig. 4 – b with average size around 300 Å could be attributed

to the large Cr oxides, but an investigation to significantly lower *Q* values would be necessary to check it. In this regard, it is stressed how important it is to extend the SANS measurements of such complex materials on a *Q*-range as wide as possible: two orders of magnitude in *Q* have been spanned, but extending the measurements to $Q = 10^{-3}$ Å^{-1} or below would allow for a more accurate characterization of the large precipitates in the different samples. On the other hand, limiting the
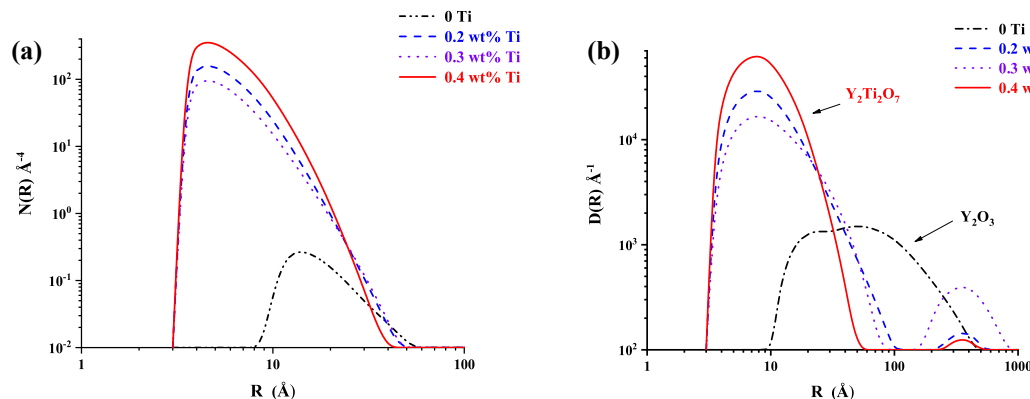

Fig. 4. Size (a) and volume (b) distributions for ODS ferritic steel with Cr 13.5 wt% W 2.0 wt% and with 0 Ti (dash-dots, black), 0.2 wt% Ti (dashes, blue), 0.3 wt% Ti (dots, violet), 0.4 wt% Ti (continuous line, red). The uncertainty error bands are below 3%.

Table 2

Volume fractions and average radii attributed to $Y_2Ti_2O_7$ nano-clusters as a function of Ti content for W content 2.0 wt%. In the reference, Ti free sample they are attributed to Y_2O_3.

Sample	volume fraction, f	average radius, $<R>$
0 Ti	0.012	24.2 Å
0.2 Ti wt%	0.021	6.6 Å
0.3 Ti wt%	0.021	6.8 Å
0.4 Ti wt%	0.032	6.5 Å

measurements to 2 m sample-to-detector distance ($Q > 4\,10^{-2}\,\text{Å}^{-1}$, see Fig. 2 – a), the complexity of the effective SANS cross-sections, and of the related micro-structures, would have been mostly lost.

5. Conclusions

Laboratory heats of mechanically alloyed 13.5 ferritic ODS steel have been investigated by SANS measurements and related data analysis, to contribute in characterizing their complex micro-structure with results complementary to those provided by electron microscopy and other local techniques. The obtained results show clearly that adding Ti to a matrix containing Y_2O_3 0.3 wt% and W 2.0 wt% a population of defects as small as approximately 12 Å in size develops, tentatively identified $Y_2Ti_2O_7$; under this assumption a volume fraction increase from 0.021 to 0.032 is observed when increasing the Ti content from 0.2 wt% to 0.4 wt%. For the Ti free sample and for a Ti content of 0.3 wt% the SANS measurements show a marked dependence of the defect composition on their size, requiring additional TEM observations and more detailed information on the chemical composition of such nano-clusters for a full exploitation of the SANS data. Namely, the TEM observations presented in Ref. [6] should be extended to the same samples utilized for the SANS measurements, increasing as much as possible the number of counted precipitates and trying to catch also those smaller than 20 Å. The observed SANS effects should also be checked on a larger number of samples prepared under identical nominal conditions: as a matter of fact, the general complexity of micro-structural evolution in ODS steels [1] may be significantly increased when the preparation route is not a fully standardized one but a small-scale, experimental procedure like in the present case. The obtained results constitute anyhow a significant progress with respect to the observation of these same samples electron microscopy [6]: in fact, they reveal the presence of small nano-clusters, practically invisible by TEM, and provide useful information on their chemical composition, averaged over a macroscopic volume.

Declaration of Competing Interest

The authors declare that they have no known competing financial interests or personal relationships that could have appeared to influence the work reported in this paper.

Acknowledgements

References

[1] G.R. Odette, Recent progress in developing and qualifying nanostructured ferritic alloys for advanced fission and fusion applications, JOM 66 (2014) 2427–2441, https://doi.org/10.1007/s11837-014-1207-5.

[2] S.J. Zinkle, J.L. Boutard, D.T. Hoelzer, A. Kimura, R. Lindau, G.R. Odette, M. Rieth, L. Tan, H. Taginawa, Development of next generation tempered and ODS reduced activation ferritic/martensitic steels for fusion energy applications, Nucl. Fus. 57 (2017) 092005.

[3] G. Federici, W. Biel, M.R. Gilbert, R. Kemp, N. Taylor, N. Wenninger, European DEMO design strategies and consequences for materials, Nucl. Fusion 57 (2017) 092002.

[4] C. Capdevila, M. Serrano, M. Campos, High strength dispersion strenghtened steels: Fundamentals and applications, Mat. Sci. Techn. 30 (13) (2014) 1655–1657.

[5] C.h. Ch Eiselt, M. Klimenkov, R. Lindau, A. Möslang, Characterization of microstructural and mechanical properties of a reduced activation ferritic oxide dispersion strengthened steel, J. Nucl. Mater. 416 (2011) 30–34.

[6] P. He, M. Klimenkov, R. Lindau, A. Möslang, Characterization of precipitates in nano structured 14% Cr ODS alloys for fusion applications, J. Nucl. Mater. 428 (2012) 131–138.

[7] P. He, M. Klimenkov, A. Möslang, R. Lindau, H.J. Seifert, Correlation of microstructure and low cycle fatigue properties for 13.5Cr1.1W0.3Ti ODS steel, J. Nucl. Mater. 435 (2014) 167–173.

[8] P. He, J. Hoffmann, A. Möslang, Effect of milling time and annealing temperature on nanoparticles evolution for 13.5% Cr ODS ferritic steel powders by joint application of XAFS and TEM, J. Nucl. Mater. 501 (2018) 381–387.

[9] S.V. Rogozhkin, N.N. Orlov, A.A. Nikitin, A.A. Aleev, A.G. Zaluzhnyi, M.A. Kozodaev, R. Lindau, A. Möslang, P. Vladimirov, Nanoscale characterization of 13.5% Cr oxide dispersion sterntgthened steels with various Ti concentrations, Inorganic Materials: Appl. Res. 6 (2) (2015) 151–155.

[10] G. Kostorz, X-ray and neutron scattering, in "Physical Metallurgy", R. W. Cahn and P. Haasen Ed.s, North Holland, 1983, 793–853.

[11] M. T. Hutchings, C. G. Windsor, Industrial applications, in K. Sköld, D. L. Price Ed.s Methods of Experimental Physics, vol 23-c, Neutron Scattering, Academic, 1987, 405-482.

[12] M.H. Mathon, M. Perrut, S.Y. Zhong, Y. De Carlan, Small angle neutron scattering study of martensitic/ferritic ODS alloys, J. Nucl. Mater. 428 (2012) 147–153.

[13] R. Coppola, M. Klimiankou, R. Lindau, R.P. May, M. Valli, SANS and TEM study of Y_2O_3 paricle distributions in oxide-dispersion strenghtened EUROFER martensitic steel for fusion reactors, Physica B 350 (2004) e545–e548.

[14] R. Coppola, R. Lindau, R.P. May, A. Möslang, M. Valli, P. Vladimirov, A. Wiedenmann, SANS study of microstructural evolution in oxide strengthened EUROFER steel after heat treatments, J. of. Ph. C 251 (2010) 012052.

[15] https://www.ill.eu/users/instruments/instruments-list/d22/description/instrument-layout/.

[16] https://www.ill.eu/users/scientific-groups/large-scale structures/grasp/.

[17] M. Magnani, P. Puliti, M. Stefanon, Numerical solution of the inverse problem in the analysis of neutron small angle scattering experiments, Nucl. Inst. Meth. A 217 (1988) 611–616.

[18] R. Coppola, M. Klimenkov, R. Lindau, A. Möslang, M. Rieth, M. Valli, Micro-structural effects of irradiation temperature and helium content in neutron irradiated B-alloyed Eurofer97-1 steel, Nucl. Mat. En. 17 (2018) 40–47.

[19] R. Coppola, M. Klimenkov, Dose Dependence of Micro-voids Distributions in Low-Temperature Neutron Irradiated Eurofer97 Steel, Metals 9 (2019) 552.

[20] M. Klimenkov, R. Lindau, E. Materna-Morris, A. Möslang, TEM characterization of precipitates in EUROFER 97, Progr. Nucl. En. 57 (2012) 8–13.